

Alternative Buffer-Layers for the Growth of $\text{SrBi}_2\text{Ta}_2\text{O}_9$ on Silicon

J. Schumacher, J. C. Martínez, F. Martin, M. Maier, H. Adrian

Johannes Gutenberg - University of Mainz; Institute of Physics; 55099 Mainz; Germany

R. Raiteri, H.J. Butt

Johannes Gutenberg - University of Mainz; Institute of Physical Chemistry; 55099 Mainz; Germany

(March 7, 2000)

In this work we investigate the influence of the use of YSZ and CeO_2/YSZ as insulators for Metal- Ferroelectric-Insulator-Semiconductor (MFIS) structures made with $\text{SrBi}_2\text{Ta}_2\text{O}_9$ (SBT). We show that by using YSZ only the a-axis oriented Pyrochlore phase could be obtained. On the other hand the use of a CeO_2/YSZ double-buffer layer gave a c-axis oriented SBT with no amorphous SiO_2 inter-diffusion layer. The characteristics of MFIS diodes were greatly improved by the use of the double buffer. Using the same deposition conditions the memory window could be increased from 0.3 V to 0.9 V. From the piezoelectric response, nano-meter scale ferroelectric domains could be clearly identified in SBT thin films.

77.80.Dj, 77.84.Dy, 68.55, 81.15.Fg

I. INTRODUCTION

With the fast development of the semiconductor industry, there is nowadays a growing interest in the investigation of novel functional layers on silicon. In particular Perovskite materials have been intensively studied during the last years. That is mainly because of the large number of different physical properties observed in this class of materials. For example, we can find among perovskites, superconducting ($\text{YBa}_2\text{Cu}_3\text{O}_7$), ferromagnetic ($\text{La}_{0.67}\text{Ca}_{0.33}\text{MnO}_3$) and ferroelectric compounds ($\text{Pb}(\text{Zr}_{1-x}\text{Ti}_x)\text{O}_3$).

Due to the high reactivity of silicon with oxygen, the deposition of high quality perovskites on similar substrates is no trivial task. However during the last years, the possibility of growing crystalline perovskites on Si by Pulsed Laser Deposition (PLD) was widely demonstrated [1]. Although this technology is not yet comfortable for wide area deposition, complex heterostructures can be prepared.

More recently, because of a growing interest on the development of non-volatile memory cells, several groups concentrated their activities on the deposition of $\text{SrBi}_2\text{Ta}_2\text{O}_9$ thin films (SBT) on silicon by Pulsed Laser Deposition [2]. A large number of buffer layers like Y_2O_3 [3], SrTiO_3 , MgO [4], Si_3N_4 [5] and Al_2O_3 [6,7] have been investigated. However the formation of an amorphous SiO_2 inter-diffusion layer can hardly be controlled by the use of these buffers.

In this work, we investigate the influence of $(\text{Y}_2\text{O}_2)_x(\text{ZrO}_2)_{1-x}$ (YSZ) and CeO_2/YSZ buffer layers on the structure, surface morphology and ferroelectric properties of $\text{SrBi}_2\text{Ta}_2\text{O}_9$ thin films. The YSZ layer has been used in order to avoid the formation of SiO_2 .

First a description of the employed deposition method is described and the structural properties of the differ-

ent layers are discussed. The characteristic surface and ferroelectric domain morphologies are studied by using Atomic Force Microscopy (AFM). Finally we compare the Capacitance versus bias Voltage (CV) characteristics of Metal-Ferroelectric-Semiconductor capacitors for $\text{SrBi}_2\text{Ta}_2\text{O}_9$ layers deposited with and without buffers.

II. PLD DEPOSITION WITH DIFFERENT BUFFER LAYERS

One of the challenging problems in depositing crystalline oxide layers on Si is to avoid the spontaneous formations of SiO_2 at the interface. Thanks to the discovery of High Temperature Superconductors (HTS), a large effort was done in order to get an effective solution. This was mainly because the superconducting properties of HTS can only be obtained through a reasonable crystalline quality. Here the solution was to use a YSZ buffer layer $(\text{Y}_2\text{O}_2)_x(\text{ZrO}_2)_{1-x}$ in order to avoid the formation of SiO_2 . Later additional layers of BaZrO_3 or CeO_2 have been used in order to avoid inter-diffusion and increase the crystalline quality. From the different studies it became clear that during the deposition of the YSZ layer, Zr reacts at high temperatures with SiO_2 giving ZrO_2 and SiO [1]. The latter can be easily removed by natural sublimation which occurs at low pressures (below 10^{-6} mbar) and temperatures above 800C. The best YSZ layers are usually obtained at pressures below 10^{-5} mbar [8]. The YSZ layer has to be deposited at low pressures while the other layers need usually pressures larger than 0.3 mbar. An in-situ deposition of the different layers, at large deposition rates, can be easily achieved by Pulsed Laser Deposition (PLD). However an ex-situ deposition of perovskites on top of pre-buffered substrates is also possible [10].

Our PLD chamber was specially designed for depositing complex heterostructures. The system consists of a carousel-type holder, which allows the in-situ deposition of up to six layers. The deposition chamber has a base pressure of about 10^{-7} mbar and maximum deposition temperature of about 1000°C . A self designed computer controlled system, allows the scanning of the laser plume over an area of about $2\times 2\text{ cm}^2$.

The silicon substrates were cleaned with different steps. In order to remove organic contamination, the substrates were cleaned with a solution of H_2SO_4 and H_2O_2 . The native SiO_2 layer was etched by a standard HF solution.

The best SBT films deposited on Si were obtained at substrate temperatures of 800°C and O_2 deposition pressures of 0.8 mbar. Only at lower pressures we observed the formation of the Pyrochlore SBT phase (p-SBT). Fig. 1 shows a θ - 2θ scan of a SBT film deposited on Si. It can be observed that a small amount of the p-SBT phase is still present. From low angle x-ray diffraction we detected a 4 nm thick layer which was attributed to a SiO_2 inter-diffusion layer. Because of the amorphous SiO_2 , the SBT layer did not grow with a defined orientation. The intensities observed in Fig. 1 are consistent with the expected values for a non-oriented powder.

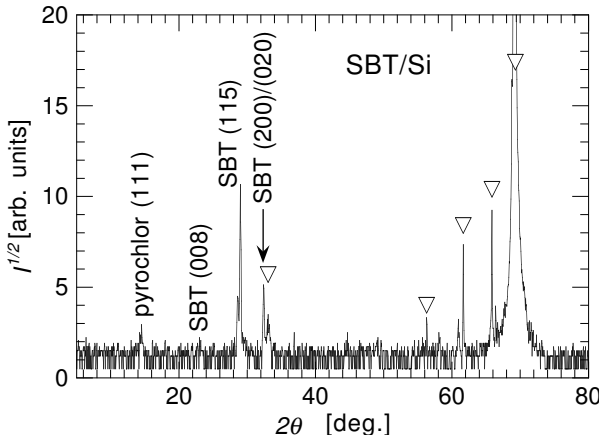


FIG. 1. X-ray diffraction in Bragg-Brentano geometry of a SBT film deposited directly on silicon. The triangles mark the reflections corresponding to the substrate.

In order to get rid of the 4 nm SiO_2 , a 40 nm thick YSZ buffer layer was deposited at typically 850°C and 10^{-5} mbar. Under these conditions the YSZ layer is c-axis oriented with rocking curves in the order of 1.2 degrees. The presence of the (111) reflection shows that a small amount of randomly oriented crystallites is still present. However, from x-ray low-angle diffraction experiments, we could not detect any SiO_2 layer.

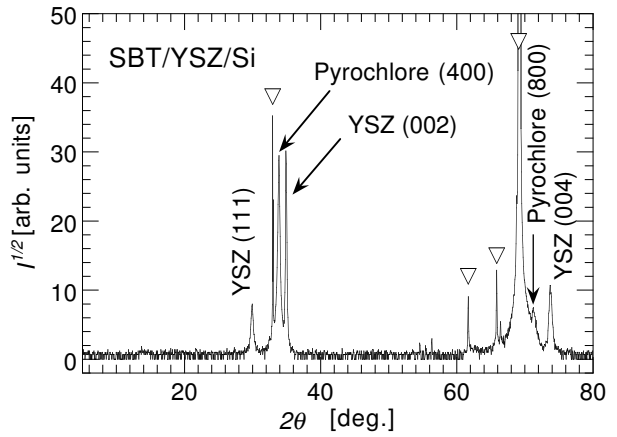


FIG. 2. X-ray diffraction of a SBT film deposited in a YSZ buffer layer. Despite the fact that the deposition parameters were identical as those in Fig. 1, we got mainly the Pyrochlore phase.

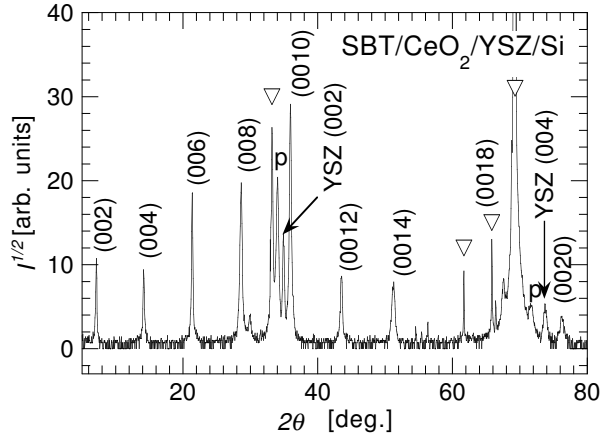


FIG. 3. SBT deposited on top of a CeO_2 /YSZ buffer shows c-axis growth with a rocking curve of 1.2° for the (006) reflection.

As we can see in Fig. 2, for the same deposition parameters for SBT as in Fig. 1, we could only grow an a-axis oriented p-SBT phase with a rocking curve of 1.4 degrees for the (400) reflex. No temperature/pressure-window could be found in order to get the desired SBT phase. This result is consistent with the work of Ishikawa et al. done on YSZ substrates [9]. As it is shown in Fig. 3, by introducing a 20 nm thick CeO_2 layer between SBT and YSZ we succeeded in obtaining a fully c-axis oriented SBT film with rocking curve of 1.2° for the (006) reflection. One can notice that only a small amount of p-SBT phase is still present. The in-plane orientation of the films was checked by Φ -scans. It can be seen that, indeed, the SBT films grow cube-to-cube with respect to the silicon substrate (Fig. 4). The biggest difficulty, in this case, was the small lattice mismatch between CeO_2 and Si, which obliged us to measure the (024) family of

reflections for CeO_2 .

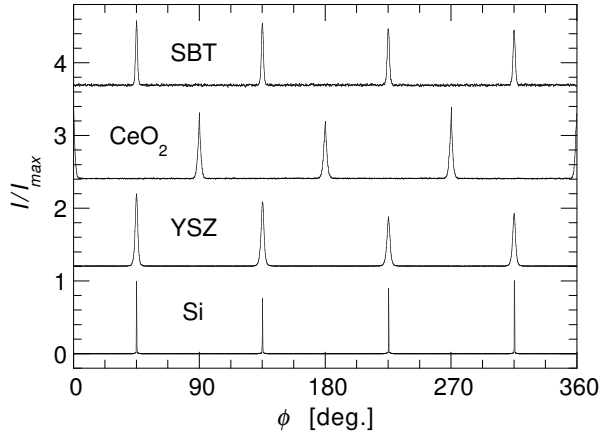


FIG. 4. Φ -scans show that SBT films grows cube to cube with respect to the silicon substrate. For SBT, YSZ and Si, we used the (111) reflexes. For CeO_2 , the (024) reflexes were taken into account because of the small lattice mismatch with respect to Si.

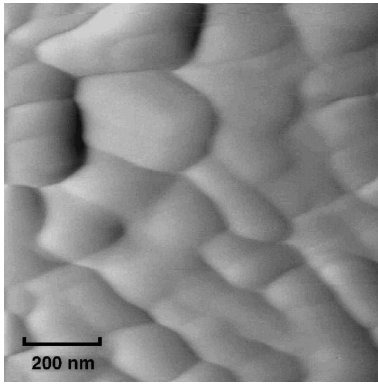


FIG. 5. AFM contact topography of a 300 nm thick SBT thin film deposited on Si. Vertical scale is 20 nm

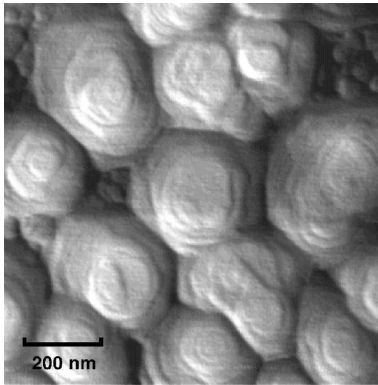


FIG. 6. AFM contact topography of a SBT/CeO₂/YSZ/Si heterostructure. The terraces correspond to unit-cell steps along the c-axis. Vertical scale is 20 nm

III. CHARACTERIZATION BY ATOMIC FORCE MICROSCOPY

We studied the topography of the different ferroelectric films with a commercial Atomic Force Microscope (AFM) [11] (Multimode, Digital Instruments, Santa Barbara, CA). The surface roughness was directly calculated from the topography images obtained in contact mode. For the SBT/Si layers we obtained an average roughness value of 5.6 nm rms (Fig. 5). An AFM image of the c-axis oriented SBT/CeO₂/YSZ/Si is shown in Fig. 6. In this case the average roughness is 4.4 nm rms. The terraces in Fig. 6 correspond to the c-axis unit cell of SBT, while the smaller grains observed at the top-right side correspond to the p-SBT phase, which could be observed in the x-ray data too.

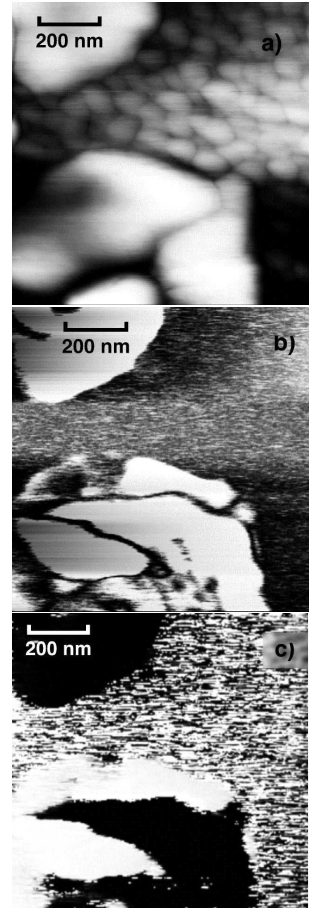


FIG. 7. AFM pictures of the same area of a SBT film grown on silicon. In this case, the film was grown at lower pressures in order to enhance the Pyrochlore phase, which corresponds to the 50 nm-wide grains in the topography image a) (z-range is 50 nm). Images b) and c) show, respectively, the amplitude and phase shift of the piezoelectric-response to an AC voltage (15 Vpp, 10 kHz). In image b) lighter colour means a higher piezoelectric response, full scale is 0.05 nm. In image c) contrast is given by relative phase shift, full scale is 180°.

In order to characterise the ferroelectric domains, an alternating voltage was applied between the conductive AFM tip and the back-side of the sample substrate during imaging, as already described in details by Martin et al. and Auciello et al. [11]. The piezoelectric response to the applied AC voltage is probed by sub-nanometer oscillations of the tip, superimposed to the static deflection kept by the AFM feedback loop. Phase shift and amplitude of the cantilever oscillation can be detected by a lock-in amplifier and recorded simultaneously with the sample topography.

Fig. 7 shows the topography, amplitude and phase shift of a 300 nm thick SBT film. This film was deposited at lower O₂ pressure (0.3 mbar) so that it is possible to observe as well the response of the 50 nm wide p-SBT grains, which appear in Fig. 7, between two large SBT grains. From the phase signal, it is possible to identify ferroelectric domains with opposite dipole orientation inside the SBT grains. In the amplitude image, we distinguish the domain walls (darker regions) between the ferroelectric domains (bright regions). The p-SBT phase shows no evident piezoelectric response.

Similar experiments done in c-axis oriented SBT films did not show features that we could directly correlate to domain structures, although, as it will be shown below, the films still showed a ferroelectric behaviour.

IV. METAL-FERROELECTRIC-INSULATOR-SEMICONDUCTOR STRUCTURES

The CV curves were found to be weakly dependent on the AC-amplitude for a range between 50 and 100 mV. The gold electrodes had a typical area of 0.5×0.5 mm².

Fig. 8 shows the capacitance versus bias Voltage U of a Au/SBT/Si heterostructure with a 300 nm thick SBT layer. The behaviour is very similar to what is expected for a Metal-Ferroelectric- Semiconductor diode measured at high frequency. Additionally the hysteresis induced by the coercive field of SBT can be observed [12]. The ferroelectricity of our isotropic SBT-film generates a typical memory window of 0.3 V.

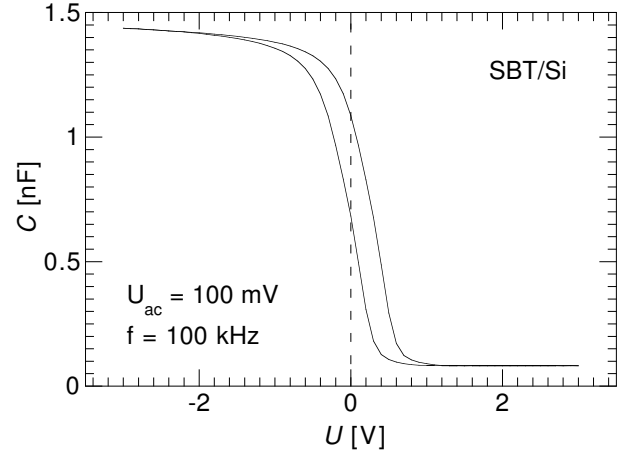


FIG. 8. Capacitance versus Voltage diagram for a metal-ferroelectric-semiconductor structure (MFS). The measurement was done at 100 kHz with AC-amplitude of 100 mV. The memory-window is 0.3 V wide

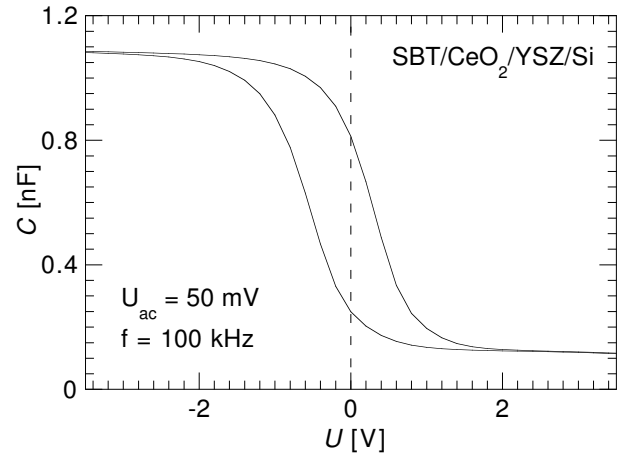


FIG. 9. Capacitance versus Voltage diagram for a Au/SBT/CeO₂/YSZ/Si heterostructure. This measurement was done at 100 kHz with AC-amplitude of 50 mV. The memory-window is 0.9 V wide.

Fig. 9 shows a CV-characteristic for a Au/SBT/CeO₂/YSZ/Si heterostructure. The thicknesses were 50, 20, and 40 nm for SBT, CeO₂, and YSZ respectively. In this case, the use of the buffer layers increased the memory window to 0.9 V. The remanent capacitance can be switched between 200 and 800 pF for voltages between ± 3 V. As it was observed by Han et al [12] and predicted by Miller and McWhorter [13], the memory window is mainly related to the coercive field and is very little influenced by the amplitude of the remanent polarization (for P_r > 0.1 C/cm²).

V. CONCLUSION

We have shown that by using CeO_2 /YSZ buffers it is possible to obtain c-axis oriented SBT films with rocking curves of 1.2° for the (006) reflection. Φ -Scans show that the films grow cube-to-cube with respect to the silicon substrate. In spite the fact that the easy direction for the polarization of SBT is known to lay along the (a,b)-plane, we observed, for c-axis SBT films, a memory window of MFIS structures of 0.9 V instead of the 0.3 V measured in Au/SBT/Si. The capacitance of the device could be switched by a factor 4 (from 200 to 800 pF) by applying 3 V.

These improvements are mainly due to the better crystalline quality of the c-axis-oriented films and the absence of amorphous SiO_2 at the YSZ/Si interface.

From AFM measurements we have been able to identify terraces which correspond to the c-axis unit cell, and we could observe ferroelectric domains in non-oriented films. For the moment we could not identify a clear domain structure in c-axis oriented SBT films.

VI. ACKNOWLEDGEMENT

J.S would like to acknowledge support from the Undergraduate Materials Research Initiative from the Materials Research Society. J.C.M and R.R were financed by the European Union under contracts (ERBM-BICT972217 and FMBICT972487). This work was partially supported by the Material Wissenschaftliches Forschung Zentrum of the University of Mainz.

- [1] E.M.Ajimine, F.E.Pagaduan, M.M.Rahman, C.Y.Yang; *Appl.Phys.Lett.* **59** 2889 (1991); C.Jaekel, C.Waschke, H.G.Roskos, H.Kurz; *Appl.Phys.Lett.* **64** 3326 (1994); Y.A.Boikov, Z.G.Ivanov, A.N.Kiselev, E.Olsson, T.Claeson; *J.Appl.Phys.* **78** 4591 (1995); L.Mchin, J.C.Villgier, G.Rolland, F.Laugier; *Physica C* **269** 124 (1996)
- [2] S.B. Desu, H.S. Cho, M.Nagata; *Phys. Stat. Solidi A* **165** 213 (1998); N.Fujimura, D.T.Thomas, S.K.Streiffer, A.J.Kingon; *Jap. Journ. Of Appl. Phys.* **37** 5185 (1998)
- [3] H.N.Lee, Y.T.Kim, S.H.Choh; *Journ. Of the Korean Phys. Soc.* **34** 454 (1999)
- [4] T.Kanashima; M.Okuyama; *Jap. Journ. Of Appl. Phys.* **38** 2044 (1999)
- [5] W.J.Lee, C.H.Shin, C.R.Cho, J.S.Lyu, B.W.Kim, B.G.Yu, K.I.Cho; *Jap. Journ. Of Appl. Phys.* **38** 2039 (1999)
- [6] W.J.Lee, B.G.Yu, J.S.Lyu, J.H.Lee, B.W.Kim, C.H.Shin, H.C.Lee; *Journ. Of the Korean Phys. Soc.* **35** S509 (1999)
- [7] Jin-Ping Han and T.P.Ma, *Appl. Phys. Lett.* **72** 1185 (1998)
- [8] D.K. Fork, S.M. Garrison, M. Hawley, T.H. Geballe, *J. Mat. Res.* **7** 255 (1992)
- [9] K. Ishikawa, N. Nukaga, K. Funakubo; *Jap.Journ.Appl.Phys.Lett.* **38** L258-L260 (1999)
- [10] J. C. Martinez, S. Ingebrandt, M. Basset, M. Mauer, M. Maier, H. Adrian; *4rth European Conference on Applied Superconductivity - EUCAS 99*; IOP Publishing Ltd; to be published
- [11] Y. Martin, D.W. Abraham, H.K. Wickramasinghe, *Appl. Phys. Lett.* **52** 1103 (1988); O. Auciello, A. Gruverman, R. Ramesh, *MRS Bulletin* **1**, **33** (1998)
- [12] J.P. Han, T.P. Ma, *Appl. Phys. Lett.* **72** 1185 (1998)
- [13] S.L. Miller and P.J. McWhorter, *J. Appl. Phys.* **72** 5999 (1992)